Mechanism of Rab Geranylgeranylation: Formation of the Catalytic Ternary Complex†

Janmeet S. Anant,‡,§ Luc Desnoyers,‡,§ Mischa Machius,§,|| Borries Demeler,⊥ Jeffrey C. Hansen,⊥ Kenneth D. Westover,‡ Johann Deisenhofer,|| and Miguel C. Seabra*,‡

Departments of Molecular Genetics and Biochemistry and Howard Hughes Medical Institute, University of Texas Southwestern Medical Center, Dallas, Texas 75235, and Department of Biochemistry, University of Texas Health Science Center, San Antonio, Texas 78284

Received April 20, 1998; Revised Manuscript Received July 8, 1998

ABSTRACT: Rab proteins are geranylgeranylated on one or two C-terminal cysteines by Rab geranylgeranyl transferase (RabGGTase). The reaction is dependent on a Rab-binding protein, termed Rab escort protein (REP). Here, we studied the role of REP in the geranylgeranylation reaction. We first characterized the interaction between REP and ungeranylgeranylated Rab using analytical ultracentrifugation and a fluorescence-based assay. We measured an equilibrium dissociation constant of 0.2 μM for the formation of a 1:1 REP−Rab complex and showed that this interaction relies mostly on ionic bonds and does not involve the two C-terminal cysteine residues. Second, we show that REP is required for recognition of Rab by RabGGTase and therefore that the REP−Rab complex is the true substrate for RabGGTase. Third, we show that free REP inhibits the geranylgeranylation reaction, suggesting that the complex is recognized by RabGGTase primarily via a REP-binding site. Our data suggest a model whereby REP behaves kinetically as an essential activator of the reaction.

Rab GTP-binding proteins regulate vesicular transport pathways in exocytic and endocytic pathways (*1*, *2*). Rab proteins require post-translational modification with geranylgeranyl (GG)[1] groups to be functionally active (*3*−*5*). This GG modification may mediate specific interactions of Rab proteins with intracellular membranes or key proteins in the Rab signaling pathway.

The enzyme that catalyzes the geranylgeranylation of Rab proteins is known as Rab geranylgeranyl transferase (RabGGTase) or GGTase type II (*6*). RabGGTase enzymatic activity requires two components, component A and component B, which were separated chromatographically during the purification of this enzyme from rat brain (*7*). Component A, now known as Rab escort protein (REP), is a soluble protein with some sequence that is similar to that of another Rab-binding protein, Rab GDI (*8*−*10*). Two REPs, REP1 and REP2, have been isolated from mammalian cells and shown to be expressed ubiquitously (*5*, *11*). Loss-of-function mutations in the REP1 gene result in a human retinal degenerative disease called choroideremia (*12*). The other component required for RabGGTase activity, component B, is now known simply as RabGGTase since it represents the enzyme per se (*6*). RabGGTase is composed of one α and one β subunit, structurally related to the corresponding subunits of the two other known protein prenyl transferases, FTase and GGTase type I (*13*).

Previous studies on FTase and GGTase type I revealed that a tetrapeptide present at the C terminus of many intracellular proteins serves as the recognition site for these prenyltransferase enzymes (*6*, *14*, *15*). This sequence, called C*AAX*, is composed of one cysteine (C), two aliphatic amino acids (*A*), and one C-terminal amino acid (*X*) that determines whether the C*AAX* sequence will be recognized by FTase (if *X* is methionine or serine) or by GGTase type I (if *X* is leucine). The C*AAX* motif is necessary and sufficient for prenylation. Recently, the crystal structure of FTase was determined, revealing that the α subunit forms a crescent-shaped double-layered seven-helix hairpin domain that envelops part of the β subunit (*16*). The β subunit is also predominantly α helical, containing an α−α barrel with six helices forming the inner barrel and six additional helices forming the outer barrel. The bottom of the barrel is shielded by loop structures, whereas the top end is open to the solvent. A cleft formed by the interface of the α and β subunits is believed to contain the peptide (C*AAX*) binding site. The deep cleft in the β subunit is lined by conserved aromatic amino acids and postulated to form the binding site for the

† This work was supported by the Pew Scholars Program in the Biomedical Sciences and by NIH Grant HL20948. J.S.A. was supported by NIH Postdoctoral Fellowship EY06677. L.D. was supported by an MRC of Canada postdoctoral fellowship. K.D.W. was supported by a Summer Undergraduate Research Fellowship. M.C.S. is a Pew Scholar.

* To whom correspondence should be addressed: Molecular Genetics, Division of Biomedical Sciences, Imperial College School of Medicine, London SW7 2AZ, U.K. Telephone: 44-171-5943024. Fax: 44-171-5943100. E-mail: m.seabra@ic.ac.uk.

‡ Department of Molecular Genetics, University of Texas Southwestern Medical Center.

§ These authors contributed equally to this work.

|| Department of Biochemistry and Howard Hughes Medical Institute, University of Texas Southwestern Medical Center.

⊥ University of Texas Health Science Center.

[1] Abbreviations: GG, geranylgeranyl; GGPP, geranylgeranyl pyrophosphate; FPP, farnesyl pyrophosphate; RabGGTase, Rab geranylgeranyl transferase; REP, Rab escort protein; FTase, farnesyl transferase; GGTase type I, geranylgeranyl transferase type I; GDI, GDP dissociation inhibitor; Mant, *N*-methylanthraniloyl; DTT, dithiothreitol.

S0006-2960(98)00881-2 CCC: $15.00
Published on Web 08/21/1998

secondary substrate, farnesyl pyrophosphate (FPP).

Unlike the two C*AAX* prenyl transferases, RabGGTase has a more complex protein substrate recognition and enzymatic reaction mechanism. By itself, Rab is not prenylated in vitro; it requires the accessory factor REP. In addition, most Rab proteins are modified with two, rather than one, GG groups on each of two C-terminal cysteine residues generally present in CC or C*X*C motifs (where *X* is any amino acid) (*17*, *18*). Although not much is known about the details of Rab protein geranylgeranylation, preliminary mechanistic studies on RabGGTase reported to date indicate that (i) REP is absolutely required for Rab geranylgeranylation (*10*); (ii) REP is a Rab-binding protein that forms stable complexes with both unprenylated Rab and prenylated Rab (Rab-GG) (*19*); (iii) REP is consumed in the reaction with the formation of stable REP−Rab-GG complexes (*19*, *20*); (iv) detergent micelles or phospholipid vesicles serve as nonspecific Rab-GG acceptors, enabling the regeneration of free REP and multiple rounds of Rab geranylgeranylation (*20*); and (v) digeranylgeranylated Rab (Rab-diGG) is the final product of the reaction (*18*).

In this report, we describe thermodynamic and kinetic studies on the formation of the catalytic complex in the Rab prenylation reaction cascade. We studied how REP interacts with Rab proteins and its role in the formation of the catalytic complex. We present evidence that it is the complex between REP and Rab which is the true substrate for RabGGTase and that this complex is primarily recognized by RabGGTase via a REP-binding site.

MATERIALS AND METHODS

Materials. All chemicals were reagent grade. Guanine nucleotides were from Boehringer Mannheim; methylisatoic anhydride was from Acros, triethylammonium bromide from Sigma, and Nonidet P-40 (protein grade) from Calbiochem. All-*trans*-[1-^{3}H]GGPP (20 Ci/mmol) was purchased from NEN-DuPont. All solutions were made with MilliQ water.

Production of Recombinant REP1 and REP2 in Sf9 Cells. REP1 and REP2 proteins containing six histidine residues at the C termini were prepared as follows (*21*). Infected Sf9 cells were lysed by sonication with three pulses of 10 min in buffer A [50 mM HEPES/NaOH, 100 mM NaCl, 1 mM β-mercaptoethanol, 5 μg/mL pepstatin, 5 μg/mL leupeptin, and 5 μg/mL aprotinin (pH 7.2)] and centrifuged at 100000*g* for 1 h at 4 °C. The supernatant was filtered through a 0.45 μm syringe-end filter and analyzed using nickel−Sepharose chromatography. The His-tagged REP1 and REP2 proteins were eluted with an imidazole gradient and dialyzed against two changes of buffer B [50 mM HEPES/NaOH, 100 mM NaCl, 5 mM $MgCl_2$, and 1 mM DTT (pH 7.2)]. After dialysis, proteins were concentrated to a final volume of 2 mL using a Centriprep30 concentrator (Amicon) (1500*g* at 4 °C) and loaded on a Superdex200 FPLC column (Hi-Load 16/60, Pharmacia). The column was equilibrated in buffer B and eluted at a flow rate of 1 mL/min. The active monomeric REP elutes at 40−45 mL. These fractions were collected, pooled, concentrated with Centriprep30 concentrator, and stored at −70 °C. The final concentration of REP was usually between 1 and 2 mg/mL.

Production of Recombinant Rab Proteins in Escherichia coli. Rab proteins containing six histidine residues at the N termini were prepared as follows (*21*). Transformed BL21 (DE3) *E. coli* cells were lysed using a French press in buffer C [20 mM Tris/HCl, 0.5 M NaCl, and 1 mM β-mercaptoethanol (pH 7.9)] and centrifuged at 30000*g* for 1 h at 4 °C. The supernatant was filtered through a 0.45 μm syringe-end filter and analyzed using nickel−Sepharose chromatography. The His-tagged Rab proteins were eluted with an imidazole gradient, dialyzed against two changes of buffer B, concentrated to a final volume of 2 mL using a Centriprep10 concentrator (Amicon) (2000*g* at 4 °C), and loaded on a Superdex75 FPLC column (Hi-Load 16/60, Pharmacia). The column was equilibrated in buffer B and eluted at 1 mL/min. The monomeric Rab fractions were collected, pooled, concentrated with a Centriprep10 concentrator, and stored at −70 °C. The final concentration of Rab proteins was usually between 1 and 2 mg/ml.

Synthesis and Purification of Mant-GDP and Mant-GMPPNP. *N*-Methylanthraniloyl (Mant) nucleotides were synthesized as described by Hiratsuka (*22*). Guanine nucleotide (1 mmol) was dissolved in a minimum amount of water (15 mL) at 38 °C, and the pH of the solution was adjusted to 9.6 with NaOH. A crystalline preparation of methylisatoic anhydride (3 mmol) was added to this solution while the mixture was stirred continuously. The pH was maintained at 9.6 by titration with 2 N NaOH for 2 h. The reaction mixture was then centrifuged, and the colored supernatant was filtered through Whatman no. 1 paper to remove particulates. The reaction mixture (maximum of 1 mL) was loaded onto a 15 mL Q-Sepharose (High Performance, Pharmacia) FPLC column, and guanine nucleotides were eluted with a linear gradient from 0.2 to 0.6 M triethylammonium bromide over 120 min. Fractions of 1 mL were collected, and 10 μL of the guanine nucleotide fractions was analyzed using MonoQ chromatography in a SMART System (Pharmacia Biotech), as described previously (*23*). The purity of Mant-GDP and Mant-GMPPNP was determined by quantitating the area of the nucleotide peaks on the corresponding chromatograph and was consistently greater than 95%.

Nucleotide Loading of Rab Proteins. Rab proteins were loaded with specific nucleotides using a procedure described previously (*23*). The efficiency of loading, which was consistently greater than 90%, was determined by analyzing the bound nucleotide using MonoQ chromatography in a SMART System (Pharmacia), as described previously (*23*).

Protein Concentration Determination. Protein concentrations were determined by UV absorption or the Bradford technique. For REP2 and Rab1a, extinction coefficients at 280 nm of 53 600 and 32 400 M^{-1} cm^{-1}, respectively, were determined with the Edelhoch method as described by Pace et al. (*24*). For Mant-labeled proteins, an extinction coefficient of 5700 M^{-1} cm^{-1} at 350 nm was used (*22*).

Fluorescence Measurements. Steady-state fluorescence measurements were performed using a Perkin-Elmer LS50 B spectrofluorimeter in the photon-counting mode. Experiments were generally carried out at 20 °C in a Quartz cuvette with a path length of 1 cm while the mixture was constantly stirred. All samples were filtered (0.22 μm) or centrifuged prior to being used. If necessary, fluorescence readings were corrected for dilution and the inner filter effect using the following formula (*25*)

$$F_{corr} = F_{obs}\frac{V}{V_0} \times 10^{0.5dA_\lambda} \quad (1)$$

where F_{corr} is the corrected fluorescence intensity value, F_{obs} is the experimentally measured fluorescence intensity, V is the volume of the sample, V_0 is the initial volume of the sample, d is the path length of the cuvette, and A_λ is the absorption of the sample at the excitation wavelength. Samples containing the Mant-labeled Rab proteins were excited at wavelengths between 360 and 380 nm, and emission spectra were recorded between 400 and 500 nm using a 390 nm cutoff filter to minimize scattering contributions. Slit widths were 5 nm for excitation and 10 nm for emission. Usually, four spectra taken with a scan speed of 200 nm/min were averaged.

REP−Rab Binding Assay. The stoichiometry and affinity of Rab binding to REP were determined by titrating fixed amounts of Rab[Mant-GDP] with varying concentrations of REP in buffer B, unless otherwise stated. Mant fluorescence emission was measured at the peak maximum of 437 nm with excitation at 381 nm. No background fluorescence could be detected in the absence of Mant nucleotide. The binding data were fitted by nonlinear regression using the programs KaleidaGraph (Synergy Software) and Mathematica (Wolfram Research) to the following formula describing a bimolecular association reaction:

$$F = F_{max}\left[K_d + M_{Rab}[Rab_0] + M_{REP}[REP] - \sqrt{(K_d + M_{Rab}[Rab_0] + M_{REP}[REP])^2 - 4M_{Rab}[Rab_0]M_{REP}[REP]}\right] \Big/ [2M_{Rab}[Rab_0]] \quad (2)$$

where F is the (corrected) experimental fluorescence value, F_{max} is the maximum fluorescence value, K_d is the dissociation constant, $[Rab_0]$ and [REP] are the total concentrations of the reactants, and M_{Rab} and M_{REP} are correction terms accounting for uncertainties in the concentrations of the reactants. The fitted parameters were F_{max}, K_d, M_{Rab}, and M_{REP}. This formula is based on the general solution for a bimolecular association reaction (*26*). The formula does not contain concentration correction factors since one assumes that the concentrations of the reactants are accurately known. However, protein concentration determination methods may vary widely in accuracy, and phenomena like oligomerization and aggregation may reduce the concentration of active material. Nevertheless, the information content of binding curves is high enough to allow fitting of the correction terms provided several titrations are performed with varying concentrations of the reactants and the same stock solutions are used within a time span where the composition of the stock solutions does not significantly change. In this study, the correction terms obtained by the fitting procedure were between 0.5 and 2, indicating at most a 2-fold error in the concentration of the reactants.

Analytical Ultracentrifugation. Sedimentation velocity and sedimentation equilibrium experiments were performed using a Beckman XL-A analytical ultracentrifuge equipped with scanning absorption optics. All experiments were carried out in 1.2 cm path length double-sector cells with Quartz windows at various speeds and temperatures between 4 and 8 °C in buffer B. Protein concentration profiles were determined by UV absorption scans along the centrifugation radius at a single wavelength (around 280 nm). Data from sedimentation equilibrium experiments were analyzed by nonlinear least-squares fitting techniques against various models describing the oligomeric status of REP in solution. Data from sedimentation velocity experiments were analyzed by the method of van Holde and Weischet (*27*). The partial specific volumes of the sample proteins were calculated on the basis of the amino acid composition and were 0.727 cm^3/g for both proteins.

In Vitro Geranylgeranylation Assays. RabGGTase activity was determined by measuring the incorporation of [^{3}H]GGPP into Rab proteins as described previously with minor modifications (*23*). Briefly, the standard reaction mixture contained the following components in a final volume of 25 μL: 50 mM HEPES/NaOH (pH 7.2), 5 mM $MgCl_2$, 1 mM DTT, 4 μM [^{3}H]GGPP (3000 dpm/pmol), and varying concentrations of recombinant Rab proteins, RabGGTase and REP1 or REP2. After incubation for 10 min at 37 °C, the reaction was stopped by the addition of 1 mL of ethanol/HCl (90:10, v/v). After 30 min, the precipitable radioactivity was measured by filtration on a 1.2 μm glass fiber filter and scintillation counting. The resulting data were fitted by nonlinear regression to equations describing general Michaelis−Menten kinetics using the program Kaleidagraph (Synergy Software).

Single-Turnover Prenylation. The single-turnover prenylation experiments were carried out essentially as described above, except that RabGGTase was preloaded with [^{3}H]-GGPP and no additional GGPP was present in the reaction mixture. To preload the enzyme, RabGGTase (100 pmol) was incubated with [^{3}H]GGPP (400 pmol) for 10 min at 25 °C in 100 μL of 10 mM potassium phosphate (pH 7.4) followed by incubation on ice for 10 min. Two hundred microliters of a continuously stirred hydroxyalkoxypropyl dextran 50% suspension (v/v) in 10 mM potassium phosphate buffer (pH 7.4) was added, and the tubes were kept on ice and vortexed every 10 min. After 30 min, the samples were centrifuged at 15000*g* for 4 min, and the supernatant containing the RabGGTase loaded with [^{3}H]GGPP was collected. Two microliters of this supernatant was then quickly added to a prenylation mixture and the precipitable radioactivity counted as described above.

Substrate Inhibition Studies. The inhibitory effect of REP on the prenylation reaction was determined by performing in vitro prenylation assays in the presence of high concentrations of REP. For the estimation of the affinity of free REP for RabGGTase (termed K_{EA}), the data were fitted using the following formula assuming that free REP acts as a competitive inhibitor (*28*):

$$v = V_{max}\frac{[REP{-}Rab]}{K_{SA}\left(1 + \frac{[REP_{free}]}{K_{EA}}\right) + [REP{-}Rab]} \quad (3)$$

where v is the velocity of the prenylation reaction, V_{max} is the maximum velocity, K_{SA} is the Michaelis−Menten constant for the substrate, and K_{EA} is the dissociation constant for the competitive inhibitor REP_{free}. The concentrations of REP−Rab and REP_{free} were calculated using the equilibrium dissociation constant established by the fluorescence titration

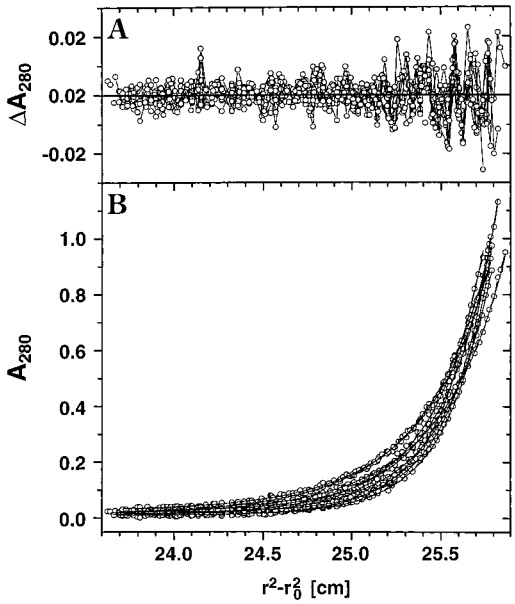

FIGURE 1: Equilibrium sedimentation analysis of REP1. REP1 (3.7, 4.7, and 5.7 μM) was subjected to ultracentrifugation in buffer B (see Materials and Methods) at three different speeds (15 000, 17 000, and 19 000 rpm) and a temperature of 4 °C (A). Data were fitted to an equation describing a monomer−dimer equilibrium using a partial specific volume of 0.727 cm^3/g and a density for the buffer of 1.004 g/cm^3 (at 20 °C). Panel B shows the residuals of the fit.

experiments according to the following formulas (*26*):

$$[\text{REP}-\text{Rab}] = {}^1/_2[K_d + [\text{REP}_0] + [\text{Rab}_0] - \sqrt{(-K_d - [\text{REP}_0] - [\text{Rab}_0])^2 - 4[\text{REP}_0][\text{Rab}_0]}] \quad (4)$$

$$[\text{REP}_{free}] = [\text{REP}_0] - [\text{REP}-\text{Rab}] \quad (5)$$

where $[\text{REP}_0]$ and $[\text{Rab}_0]$ are the initial concentrations of the reactants and K_d is the dissociation constant.

RESULTS

REP Is Monomeric in Solution. REP exhibits anomalous behavior on SDS−PAGE under reducing conditions where it has an electrophoretic mobility corresponding to a particle with apparent molecular mass of about 95 kDa (*10*), although the molecular mass is only 72 kDa on the basis of its nucleotide sequence. On gel filtration chromatography, REP has a Stokes radius corresponding to a globular particle with an apparent molecular mass of about 150 kDa (data not shown), indicating that its shape deviates significantly from a sphere or that it exists as a dimer. To resolve this question, we have undertaken analytical ultracentrifugation studies. Figure 1 shows sedimentation equilibrium profiles for REP. The data correspond very well to a model for a reversible monomer−dimer equilibrium with a dissociation constant of 4.9 μM and a molecular mass of 77 kDa for the monomer. The results suggest that REP is essentially monomeric in solution, but has a slight tendency to dimerize.

REP−Rab Interaction Studied with Fluorescence Spectroscopy. It has been shown for many nucleotide binding proteins that fluorescent nucleotide analogues can be used to probe their interaction with other proteins. We investigated the possibility of using the fluorescent GDP analogue Mant-GDP bound to the Rab proteins as a reporter molecule

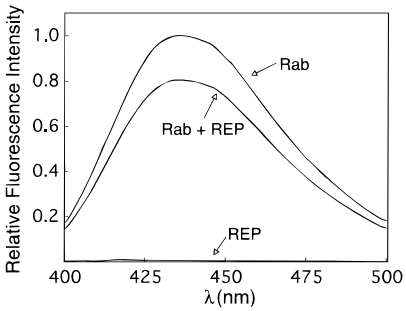

FIGURE 2: REP-induced quenching of Rab[Mant-GDP] fluorescence. Rab1a[Mant-GDP] (80 nM) with or without 1 μM REP2 or 1 μM REP2 without Rab1a[Mant-GDP] was incubated and subjected to fluorescence analysis as described in Materials and Methods. The samples were excited at 365 nm, and the emission intensity was measured from 400 to 500 nm.

for the quantitative characterization of the interaction between REP and Rab proteins in solution. After exchanging the nucleotides intrinsically bound to recombinant unprenylated Rab1a, we investigated if the Mant-labeled nucleotide influenced the overall biochemical properties of Rab1a. We subjected Rab1a[Mant-GDP] to the in vitro prenylation reaction described in Materials and Methods and observed that Rab1a[Mant-GDP] was as effective as Rab1a[GDP] in the prenylation reaction (data not shown).

We then studied the effect of REP−Rab interaction on the intrinsic Mant fluorescence of unprenylated Rab1a[Mant-GDP]. Figure 2 shows fluorescence emission spectra of Rab1a[Mant-GDP] before and after adding REP2. The addition of REP2 to unprenylated Rab1a[Mant-GDP] results in a quenching of the Mant-GDP fluorescence of up to approximately 25%. We also observed that REP binding does not alter the Mant-GDP emission maximum which suggests that REP2 binding to Rab1a changes the electronic characteristics around the Mant fluorophore, but does not influence the hydrophobicity of its surroundings.

Specificity of REP-Induced Fluorescence Quenching. We tested the specificity of the observed quenching effect in several ways, as follows. RabGDI is a well-characterized Rab-binding protein sharing structural homology with REP (*29*). In contrast to REP, however, there is evidence that RabGDI binds to Rab proteins only when they are prenylated (*8*). When equivalent amounts of RabGDI were added to unprenylated Rab[Mant-GDP], no detectable changes in the Mant-derived fluorescence intensity could be observed (Figure 3B). As an additional control, we loaded Rab1a with the fluorescently tagged GTP analogue, Mant-GMPPNP, and observed that REP could no longer induce quenching (Figure 3C). This result is consistent with our previous studies showing that REP binds poorly to Rab[GTP] (*23*). Finally, since REP is known to bind Rab but not other related GTPases such as Ras, we show that REP does not induce quenching when incubated with H-Ras[Mant-GDP] (Figure 3D). While we cannot rule out the possibility that these negative results are due to a lack of induced quenching rather than a lack of binding, the most likely interpretation is that the assay is measuring specific binding of REP to Rab[GDP]. To further ensure that the fluorescence quenching was induced by REP binding, we performed a competition experiment. We first titrated REP to quench the Rab[Mant-GDP] fluorescence and then added a 10-fold molar excess of unlabeled Rab[GDP]. We observed that the decrease in

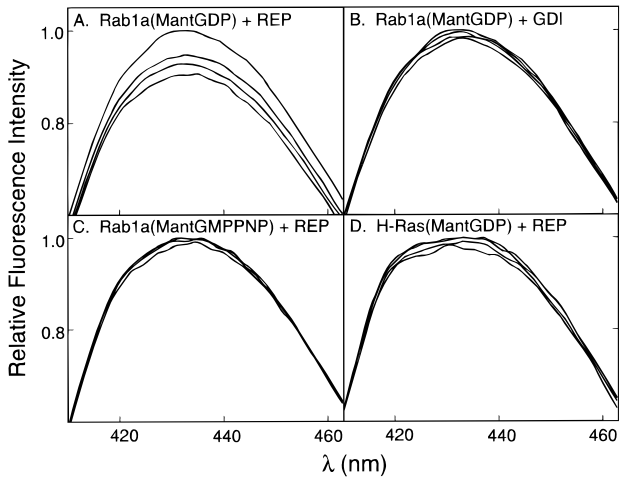

FIGURE 3: Specificity of the REP−Rab fluorescence quenching assay. Three consecutive 160 nM aliquots of REP1 (A, C, and D) or RabGDI (B) were added to a solution of 80 nM Rab[Mant-GDP] (A and B), Rab[Mant-GMPPNP] (C), or H-Ras[Mant-GDP] (D), and the mixtures were incubated and subjected to fluorescence analysis as described in Materials and Methods. The samples were excited at 365 nm, and the emission intensity was measured from 400 to 500 nm.

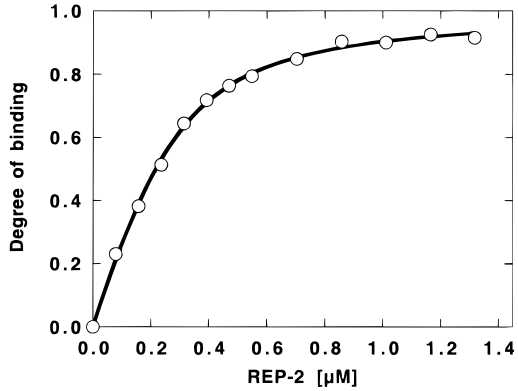

FIGURE 4: Measurement of the REP−Rab dissociation constant. Consecutive 160 nM aliquots of REP2 were added to a solution of 80 nM Rab[Mant-GDP] and the mixtures subjected to fluorescence analysis as described in Materials and Methods. The sample was excited at 365 nm, and the emission intensity at 437 nm was measured. The changes in fluorescence were normalized for dilution of the sample and plotted as the normalized change in fluorescence ($-\Delta F/F_o$, where F_o is the initial fluorescence intensity before addition of REP2) vs the concentration of REP2 (nanomolar). The data were fitted as described in Materials and Methods.

signal intensity was rapidly reversed, approaching the initial fluorescence intensity of Rab[Mant-GDP] (data not shown). However, when a 10-fold molar excess of Rab[GMPPNP] was used in the competition experiment, no reversal of the fluorescence quenching was detected (data not shown). Together, the data suggest that quenching is a specific consequence of REP−Rab interaction and is a useful readout assay for studying its properties.

Stoichiometry and Affinity of the REP−Rab Interaction. Earlier studies demonstrated that REP and Rab proteins interact with each other (*19*, *20*), but the stoichiometry and the affinity of this interaction were not quantified since a suitable method for the detection of the interaction in solution under equilibrium conditions was not available. The Mant-GDP fluorescence quenching assay allowed us to record accurate binding curves and determine both the stoichiometry and the dissociation constant for this interaction. The binding data shown in Figure 4 could be modeled after a bimolecular association reaction (i.e., 1:1 stoichiometry) with excellent statistical agreement. Furthermore, the data from several independent experiments allowed us to calculate a dissociation constant of 200 ± 40 nM for the interaction between REP2 and Rab1a[Mant-GDP].

In a complementary study, we subjected REP1, Rab1a, and a mixture of REP1 and Rab1a to sedimentation velocity experiments. For the mixture, the concentrations of REP and Rab were equimolar and chosen such that the degree of binding was 0.5 based on the parameters derived from the fluorescence experiments. Figure 5 shows sedimentation velocity boundaries and results obtained from an analysis like that of van Holde and Weischet (*27*, *30*). Under the conditions used, Rab1a behaves almost ideally monomerically with a sedimentation coefficient of 2.2 S (data not shown). For REP, the tendency to dimerize, as characterized by the sedimentation equilibrium described above, can clearly be seen in the sedimentation velocity experiment as well. The REP monomer has a sedimentation coefficient of 4.2 S (Figure 5B). For the complex between REP and Rab, the boundary fraction profile (Figure 5D) shows that about 50% of the particles present in the mixture have a sedimentation coefficient of 5.1 S, corresponding very well to a 1:1 REP−Rab complex and consistent with the thermodynamic parameters determined by the fluorescence titration experiments.

Characterization of the REP−Rab Interaction. The fluorescence-based binding assay gave us a convenient method for studying the interaction between REP and Rab under a variety of conditions. We found that high ionic strength (500 mM NaCl) reduces REP−Rab affinity by a factor of almost 10 (Table 1), while the presence of up to 10 mM nonionic detergent NP-40 had no significant effect (Table 1). The fluorescence properties of Rab1a[Mant-GDP] in the absence of REP were not influenced by high ionic strength, ruling out possible artifactual fluorescence quenching effects. The data suggest that REP−Rab interaction prior to prenylation is stabilized mainly by polar forces.

We also examined the REP-binding ability of a mutant Rab1a where both carboxy-terminal cysteines are mutated to serines (Rab1a-SS). Rab1a-SS is unable to undergo prenylation since prenyl addition occurs at the C-terminal cysteines. We found that Rab1a-SS binds with an affinity similar to that of wild type Rab1a (Rab1a-CC), confirming previous suggestions that REP binds Rab through regions distant from the site of prenylation and explaining the ability of Rab1a-SS to compete for Rab1a wild type prenylation (*20*).

Differential Interaction between REP and Rab Proteins. Given the fact that there are two REP proteins, REP1 and REP2, and a family of more than 40 different Rab proteins that serve as substrates in the prenylation reaction catalyzed by RabGGTase, we were interested in studying the interaction of different Rab proteins with both REPs. In Table 1, we show the summary of the results. We found that REP1 and REP2 bind with approximately the same affinity (ranging between 200 and 400 nM) to two different Rab proteins, Rab1a and Rab5a. These data are consistent with previous suggestions that REP1 and REP2 are functionally redundant and can aid in the prenylation of multiple Rab proteins.

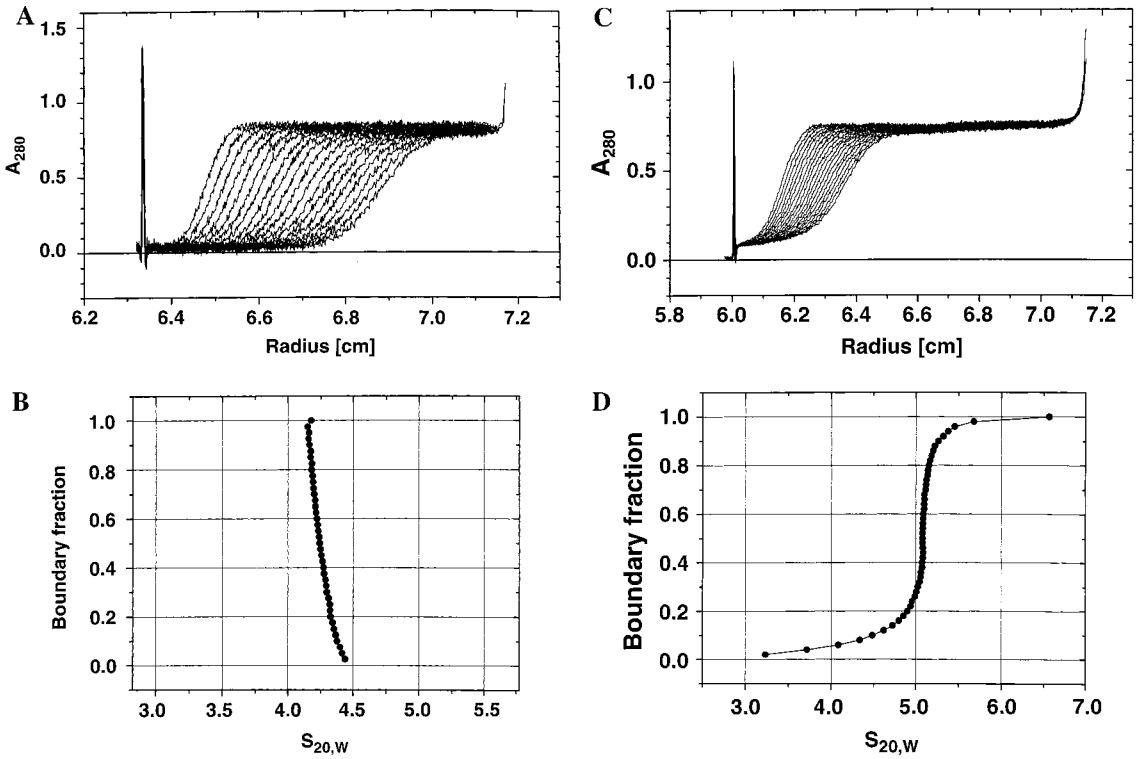

FIGURE 5: Analysis of sedimentation velocity boundaries of REP1 and REP1−Rab1a by the method of van Holde and Weischet (*27*). REP1 (A and B) and a mixture of REP1 and Rab1a (C and D) were subjected to ultracentrifugation under the following experimental conditions: REP1, 0.5 μM, speed of 60 000 rpm; REP1 and Rab1a mixture, 0.5 μM REP1 and Rab1a, speed of 60 000 rpm. The partial specific volume was 0.727 cm^3/g for all samples, and the temperature was 4.5 ± 0.5 °C. The sedimentation velocity boundaries used for the analyses are shown in panels A and C. Extrapolation plots are not shown. Integral distributions of *s* plots are shown in panels B and D (*30*).

Table 1: Comparison of Equilibrium Constants for Dissociation of REP1 or REP2 from Different Rab Proteins

REP	Rab	[NaCl] (mM)	[NP-40] (mM)	K_d (nM)
REP1	Rab1a-CC	−	−	150 ± 5
REP1	Rab1a-CC	100	−	180 ± 10
REP1	Rab1a-CC	200	−	400 ± 10
REP1	Rab1a-CC	500	−	1200 ± 140
REP1	Rab1a-CC	100	0.1	320 ± 100
REP1	Rab1a-CC	100	1	310 ± 80
REP1	Rab1a-CC	100	10	320 ± 100
REP1	Rab1a-SS	100	−	290 ± 30
REP1	Rab5a	100	−	420 ± 130
REP2	Rab1a-CC	100	−	350 ± 130
REP2	Rab1a-SS	100	−	290 ± 20
REP2	Rab5a	100	−	340 ± 50

Role of REP in the Prenylation Reaction. After characterization of the REP−unprenylated Rab association, we clarified the role of REP in the formation of the catalytic complex with RabGGTase. Previous studies suggested that REP acts prior, during, and after prenylation because steady-state prenylation is dependent on REP and that REP binds both unprenylated and prenylated Rab. However, the central unresolved question was whether the REP−Rab complex is the true substrate for RabGGTase. We sought to address this question by examining the requirement for REP in one-turnover reactions. For this purpose, we first loaded RabGGTase with GGPP. As shown previously for the C*AAX* prenyltransferases, we found recently that RabGGTase binds stably to GGPP in the absence of Rab (*34*). Therefore, we formed a RabGGTase−[^{3}H]GGPP complex that was then incubated with Rab in the presence or absence of REP. As shown in Figure 6, there is no transfer of GG to Rab unless

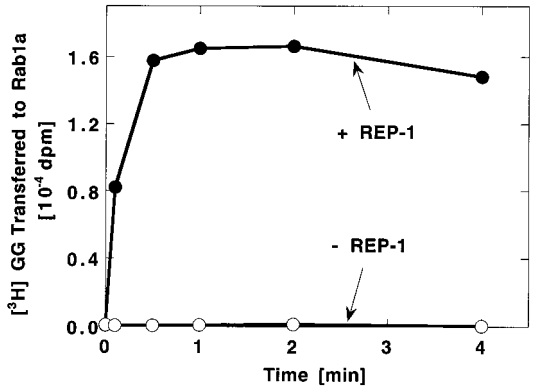

FIGURE 6: Requirement for REP in single-turnover geranylgeranylation of Rab1a. Each reaction mixture contained in a final volume of 25 μL 2 μM recombinant Rab proteins and 80 nM RabGGTase−[^{3}H]GGPP preformed complex as described in Materials and Methods. The reaction mixtures were incubated at 37 °C in the presence (●) or absence (○) of 80 nM REP1 and the reactions stopped at the indicated times (0−4 min). The amount of [^{3}H]GG transferred to Rab1a protein was determined as described in Materials and Methods. A blank value determined in the absence of Rab was subtracted from each point.

REP is present. This result rules out the possibility that the role of REP is simply to remove Rab proteins from the RabGGTase active site once it is prenylated. Instead, the data suggest that REP is absolutely required for the recognition of Rab by the RabGGTase.

Kinetics of Rab Prenylation. Having defined the affinity of REP for Rab and established that Rab is not prenylated by RabGGTase unless it is complexed with REP, we analyzed the kinetics of prenylation of REP−Rab. Previous

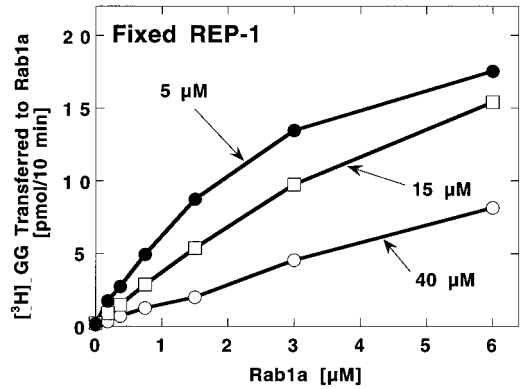

FIGURE 7: Effect of REP concentration on geranylgeranylation of Rab1a. Each reaction mixture containing in a final volume of 25 μL 4 μM [^{3}H]GGPP, 0.02 μM RabGGTase, the indicated varying concentrations of Rab1a (0−6 μM), and the indicated fixed concentrations of REP1 (5 μM, ●; 15 μM, □; and 40 μM, ○) was incubated at 37 °C for 10 min. The amount of [^{3}H]GG transferred to Rab1a protein was determined as described in Materials and Methods. A blank value determined in the absence of Rab was subtracted from each point.

steady-state reactions were performed with limiting amounts of REP and relied on REP recycling after release of prenylated Rab onto phospholipid vesicles or detergent micelles (*19*, *20*). To extract meaningful kinetic parameters, we simplified the in vitro assay by examining prenylation of Rab1a in the presence of excess REP1 (and absence of phospholipids or detergents). Surprisingly, we found that Rab1a saturation curves depended on the concentration levels of REP1 in the reaction (Figure 7). Higher concentrations of REP1 led to a right shift of the saturation curves, suggesting that free REP exerts an inhibitory effect. To test this possibility, we varied the concentration of REP1 in the presence of a fixed limiting concentration of Rab1a. As shown in Figure 8A, once free REP1 was present in the reaction mixture, we observed inhibition of Rab1a prenylation. The same effect was observed with REP2. The reverse experiment where the concentration of Rab1a was varied in the presence of a fixed limiting concentration of REP1 (or REP2) showed no inhibitory phase, even with very high (20-fold) concentrations of free Rab (Figure 8B). We conclude that free REP competes for REP−Rab prenylation possibly by forming nonproductive complexes with RabGGTase.

Table 2: Comparison of Steady-State Kinetic Constants for Different Protein Substrates of RabGGTase

substrate	K_{SA} (μM)	k_{cat} (s^{-1})[a]	k_{cat}/K_{SA} (M^{-1} s^{-1})
REP1−Rab1a	0.39 ± 0.04	0.029	74 360
REP1−Rab5a	0.31 ± 0.12	0.021	67 740
REP2−Rab1a	0.35 ± 0.05	0.025	71 430
REP2−Rab5a	0.21 ± 0.24	0.018	85 710

[a] K_{cat} values are calculated assuming transfer of two GG groups to Rab.

To determine the Michaelis constant for REP−Rab (defined as K_{SA} as described in the Discussion) in the prenylation reaction, we used substrate saturation curves of REP1or REP2 in the presence of excess fixed Rab1a to prevent inhibition from free REP (Figure 9). Using the same experimental setup, we then determined the kinetic parameters for REP1 or REP2 in complex with Rab1a or Rab5a and present the data from several independent experiments in Table 2. We found no significant differences between the different complexes, suggesting that RabGGTase can efficiently catalyze prenyl transfer to different Rab proteins bound to the two known REPs.

Substrate Inhibition of RabGGTase. Once we established that REP inhibits the prenylation reaction, we were interested in determining the affinity of free REP for RabGGTase, termed K_{EA}. We used reaction conditions similar to those used for Figure 8A, where we titrated REP in the presence of fixed limiting levels of Rab1a (Figure 10). To determine K_{EA}, we treated free REP as a competitive inhibitor. We took the inhibitory phase of the curve and fitted the data as described in Materials and Methods. We determined that K_{EA} equals 3.5 μM for REP1 and 7.0 μM for REP2.

DISCUSSION

This study reveals new mechanistic insights into the role of REP in the geranylgeranylation of Rab proteins. We adapted a widely used assay based on a fluorescent nucleotide analogue to examine REP and Rab interaction in solution. This assay is based on the quenching of the fluorescence derived from the guanine nucleotide analogue, Mant-GDP, loaded onto Rab upon binding of REP. While our studies were in progress, Cerione and colleagues published their

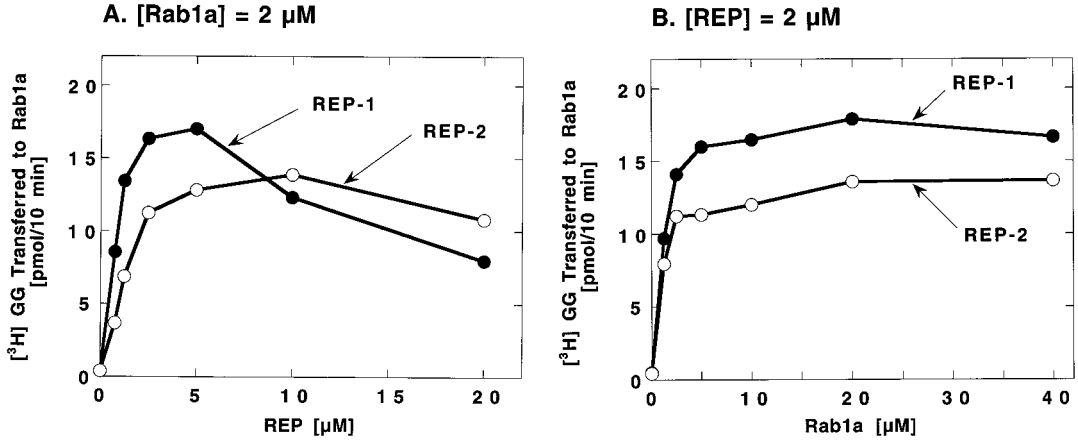

FIGURE 8: Effect of free Rab or free REP on the geranylgeranylation of Rab1a. Each reaction mixture containing in a final volume of 25 μL 4 μM [^{3}H]GGPP, 0.02 μM RabGGTase, and either a fixed concentration (2 μM) of Rab1a and various concentrations (0−20 μM) of REP1 or REP2 (A) or a fixed concentration (2 μM) of REP1 or REP2 and various concentrations (0−40 μM) of Rab1a (B) was incubated for 10 min at 37 °C. The amount of [^{3}H]GG transferred to Rab1a protein was determined as described in Materials and Methods. A blank value determined in the absence of Rab was subtracted from each point.

Scheme 1: Mechanism of the Reaction Catalyzed by RabGGTase

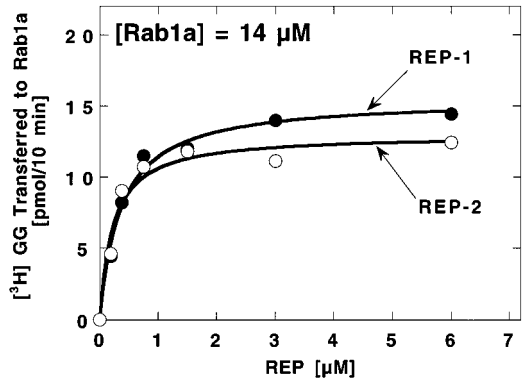

FIGURE 9: Determination of K_{SA} for REP−Rab. Each reaction mixture containing in a final volume of 25 μL 4 μM [^{3}H]GGPP, 0.02 μM RabGGTase, 14 μM Rab1a, and the indicated concentrations of REP1 (●) or REP2 (○) was incubated for 10 min at 37 °C. The amount of [^{3}H]GG transferred to Rab1a protein was determined as described in Materials and Methods. A blank value determined in the absence of Rab was subtracted from each point.

study on RhoGDI−CDC42 interaction using a similar approach, suggesting that this method may be of general use in analyzing how small GTPases interact with their regulators (*26*).

Using a combination of techniques, we were able to characterize equilibrium thermodynamic parameters for the binding of REP to unprenylated Rab proteins and showed that this interaction relies mostly on polar interactions and does not involve the two C-terminal cysteine residues. Interestingly, this complex is not disrupted by NP-40. However, after prenylation, the REP−Rab-GG complex becomes sensitive to detergent (*20*), suggesting that the GG groups attached to Rab proteins after prenylation may be the driving force for the partitioning of prenylated Rab proteins into membranes. Furthermore, the GG moieties may contribute significantly to the binding affinity since we observed previously that the reaction stops after only one turnover when REP is limiting because REP remains bound to diGG-Rab even in the presence of excess unprenylated Rab (*19*).

The two known REP proteins do not show different binding affinities for the Rab proteins tested in this study. Although incomplete since we only tested two out of more than 40 different Rab proteins, our findings suggest that the primary interaction between REP and Rab proteins is mediated by structural motifs which can be found in all Rab proteins. There might, however, be slight differences in REP binding for some Rab proteins, since we have recently proposed that choroideremia, the human retinal degenerative disease that results from mutations in REP1, may result from the incomplete geranylgeranylation of one Rab (Rab27) that has a lower affinity for REP2 (*31*). With this study, we have laid the foundation for a systematic characterization of REP−Rab interactions which is only limited by the availability of Rab proteins.

The role of REP in the prenylation reaction was only incompletely understood, and it was the central issue of our

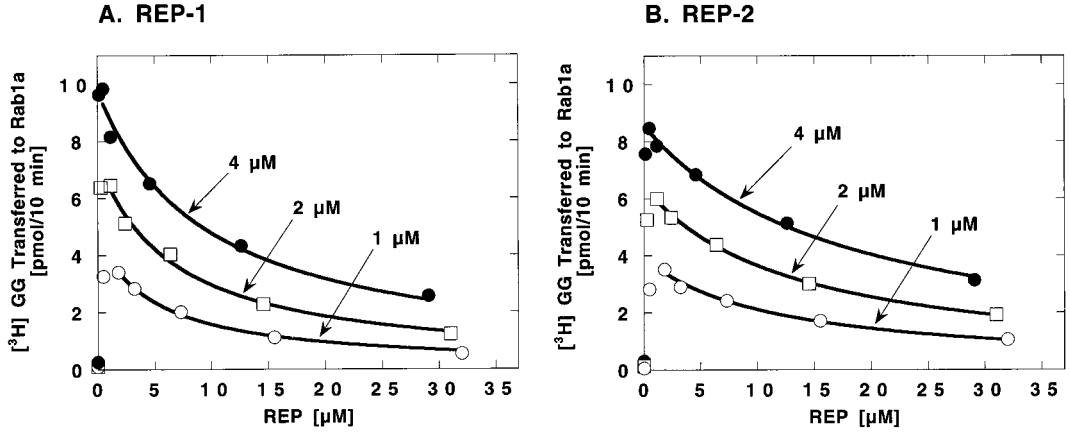

FIGURE 10: Determination of K_{EA} for free REP. Each reaction mixture containing in a final volume of 25 μL 4 μM [^{3}H]GGPP, 0.02 μM RabGGTase, three fixed concentrations of Rab1a (4 μM, ●; 2 μM, □; and 1 μM, ○) and the indicated varying concentrations of REP1 (A) or REP2 (B) was incubated for 10 min at 37 °C. The amount of [^{3}H]GG transferred to Rab1a protein was determined as described in Materials and Methods. A blank value determined in the absence of Rab was subtracted from each point. Only the inhibitory phase of each curve was fitted.

study. Using a combination of approaches (Figures 6 and 8), we present evidence that REP is required for recognition of Rab by RabGGTase and therefore that the REP−Rab complex is the true substrate for RabGGTase. In other words, it is now clear that REP should be regarded as a component of the substrate and not as a component of the enzyme. The term component A of RabGGTase, as we previously referred to it (*10*), should definitely be abandoned. The central question in this respect is now why the prenylation of Rab proteins requires the presence of REP whereas the prenylation of other small G-proteins does not require an accessory protein. The answer might lie in the nature of the prenyl modification. Rab proteins are doubly geranylgeranylated; i.e., their hydrophobic character changes dramatically upon prenylation. We hypothesize that REP is required to shield the hydrophobic geranygeranyl groups, increasing the solubility of prenylated Rab proteins, and might therefore be regarded as a specific chaperone.

The concept that REP is a component of the substrate allowed us to change our view about the prenylation reaction mechanism. Previously, we used limiting amounts of REP in our steady-state studies. Once the product REP−Rab-diGG was formed, it was disrupted (inefficiently) by phospholipid vesicles or detergent micelles. Rab-diGG translocated to vesicles or micelles most likely due to the hydrophobic character imparted by the prenyl groups, whereas REP could bind to another unprenylated Rab protein, re-entering the prenylation cycle. By carefully dissecting the individual steps leading to the formation of the catalytic complex, we could reduce the requirements for in vitro Rab prenylation to a minimum. We found that the omission of detergents or phospholipids from the reaction mixture allowed us a much more accurate determination of the catalytic efficiency of the enzyme since we measured solely the formation of REP−Rab-diGG from REP−Rab undisturbed by other processes, such as REP recycling.

A novel finding in this study was the observation that free REP inhibits the prenylation reaction. The most likely explanation for the observed effect is that free REP binds to RabGGTase and competes for binding with the REP−Rab complex. However, we cannot rule out at present the unlikely possibility that free REP is binding to a REP−Rab complex and preventing it from binding RabGGTase. If free REP is binding RabGGTase, then our data imply that the REP−Rab complex is recognized primarily via a REP-binding site on the enzyme. One interesting possibility raised by these findings is that the formation of nonproductive REP−RabGGTase complexes may regulate enzymatic activity in vivo. A consequence of this hypothesis is that excess REP is toxic to cells. In fact, we found that REP cannot be overexpressed in Sf9 cells and mammalian cells at high levels and that endogenous levels of REP are quite low, much lower than those of RabGDI (unpublished observations).

The inhibition data also suggest that there may be significant conformational changes on REP upon binding Rab since we observed a 10-fold difference between the affinity of free REP (3.5−7 μM) and the affinity of REP−Rab (0.2−0.4 μM). This possibility is further supported by the analytical ultracentrifugation experiments. We observed that both REP and Rab have relatively large Stokes radii given the molecular masses of these proteins, indicating that both proteins deviate significantly from a globular shape. It is known that small GTP-binding proteins contain a rather flexible C-terminal region, known as the hypervariable region, comprising about 70 residues that could be responsible for the observed Stokes radius (*32*). Similarly, a secondary structure prediction [PredictProtein (*33*)] for REP indicates that a large portion of about 160 residues in the middle (residues 64−223 in REP1) and another portion of about 100 residues at the C terminus of this protein do not contain regular secondary structure elements. In contrast, the complex between REP and Rab seems to be more compact compared to the individual proteins. Altogether, these results suggest that significant conformational changes accompany complex formation, which might include a (partial) ordering of the flexible regions in both proteins.

The kinetic parameters measured in this study suggest that the enzyme processes the different REP−Rab complexes with equal efficiency. The K_{cat} values obtained here are approximately 2-fold lower than the one reported for FTase. This is interesting since we calculated the K_{cat} values assuming double geranylgeranylation of the substrates. If we calculate the K_{cat} per GG group transferred assuming that the rate of transfer of the first and second GG group would be the same, then the value would be almost identical between the two protein prenyltransferases. This may represent a striking conservation of reaction mechanism between the two enzymes.

Altogether, the current evidence suggests that REP behaves mechanistically as an essential activator of the reaction (*28*). On the basis of all the current evidence, we propose the reaction mechanism depicted in Scheme 1. Free REP rapidly assembles with newly synthesized Rab to form a stable complex. Alternatively, REP binds RabGGTase nonproductively. This binding would be unlikely in vivo if there were factors promoting rapid and efficient REP−Rab interaction. Upon formation of a ternary complex, GG groups are transferred to Rab and dissociation of the product REP−Rab-diGG releases RabGGTase for another round of catalysis.

Our current model still does not describe all aspects of the prenylation reaction cascade; in particular, there is no clear understanding of the mechanisms involved in double geranylgeranylation of the Rab substrates. We have recently shown that RabGGTase has the property of binding stably to GGPP, as previously described for the other protein prenyltransferases (*34*). Furthermore, we determined that there is a single GGPP binding site on RabGGTase. These findings imply that the prenylation reaction proceeds in two independent consecutive steps. In a first step, one C-terminal cysteine is prenylated, resulting in a REP−Rab-monoGG adduct (*20*). This adduct must serve as the substrate for the second GG addition, but it is unknown whether this intermediate complex dissociates temporarily from GGTase or remains stable until double geranylgeranylation is completed. Future studies will address these issues.

ACKNOWLEDGMENT

We thank David Corey for allowing use of his equipment.

REFERENCES

1. Pfeffer, S. R. (1994) *Curr. Opin. Cell Biol. 6*, 522−526.

2. Novick, P., and Zerial, M. (1997) *Curr. Opin. Cell Biol. 9*, 496−504.
3. Kinsella, B. T., and Maltese, W. A. (1991) *J. Biol. Chem. 266*, 8540−8544.
4. Gorvel, J. P., Chavrier, P., Zerial, M., and Gruenberg, J. (1991) *Cell 64*, 915−925.
5. Desnoyers, L., Anant, J. S., and Seabra, M. C. (1996) *Biochem. Soc. Trans. 24*, 699−703.
6. Casey, P. J., and Seabra, M. C. (1996) *J. Biol. Chem. 271*, 5289−5292.
7. Seabra, M. C., Goldstein, J. L., Sudhof, T. C., and Brown, M. S. (1992) *J. Biol. Chem. 267*, 14497−14503.
8. Araki, S., Kikuchi, A., Hata, Y., Isomura, M., and Takai, Y. (1990) *J. Biol. Chem. 265*, 13007−13015.
9. Sasaki, T., Kikuchi, A., Araki, S., Hata, Y., Isomura, M., Kuroda, S., and Takai, Y. (1990) *J. Biol. Chem. 265*, 2333−2337.
10. Seabra, M. C., Brown, M. S., Slaughter, C. A., Sudhof, T. C., and Goldstein, J. L. (1992) *Cell 70*, 1049−1057.
11. Cremers, F. P., Armstrong, S. A., Seabra, M. C., Brown, M. S., and Goldstein, J. L. (1994) *J. Biol. Chem. 269*, 2111−2117.
12. Seabra, M. C., Brown, M. S., and Goldstein, J. L. (1993) *Science 259*, 377−381.
13. Armstrong, S. A., Seabra, M. C., Sudhof, T. C., Goldstein, J. L., and Brown, M. S. (1993) *J. Biol. Chem. 268*, 12221−12229.
14. Gelb, M. H. (1997) *Science 275*, 1750−1751.
15. Zhang, F. L., and Casey, P. J. (1996) *Annu. Rev. Biochem. 65*, 241−269.
16. Park, H. W., Boduluri, S. R., Moomaw, J. F., Casey, P. J., and Beese, L. S. (1997) *Science 275*, 1800−1804.
17. Farnsworth, C. C., Kawata, M., Yoshida, Y., Takai, Y., Gelb, M. H., and Glomset, J. A. (1991) *Proc. Natl. Acad. Sci. U.S.A. 88*, 6196−6200.
18. Farnsworth, C. C., Seabra, M. C., Ericsson, L. H., Gelb, M. H., and Glomset, J. A. (1994) *Proc. Natl. Acad. Sci. U.S.A. 91*, 11963−11967.
19. Andres, D. A., Seabra, M. C., Brown, M. S., Armstrong, S. A., Smeland, T. E., Cremers, F. P., and Goldstein, J. L. (1993) *Cell 73*, 1091−1099.
20. Shen, F., and Seabra, M. C. (1996) *J. Biol. Chem. 271*, 3692−3698.
21. Armstrong, S. A., Brown, M. S., Goldstein, J. L., and Seabra, M. C. (1995) *Methods Enzymol. 257*, 30−41.
22. Hiratsuka, T. (1983) *Biochim. Biophys. Acta 742*, 496−508.
23. Seabra, M. C. (1996) *J. Biol. Chem. 271*, 14398−14404.
24. Pace, C. N., Vajdos, F., Fee, L., Grimsley, G., and Gray, T. (1995) *Protein Sci. 4*, 2411−2423.
25. Lakowicz, J. R., Maliwal, B. P., Cherek, H., and Balter, A. (1983) *Biochemistry 22*, 1741−1752.
26. Nomanbhoy, T. K., and Cerione, R. (1996) *J. Biol. Chem. 271*, 10004−10009.
27. van Holde, K. E., and Weischet, W. O. (1978) *Biopolymers 17*, 1387−1403.
28. Segel, I. H. (1975) in *Enzyme Kinetics*, pp 227−273, Wiley, New York.
29. Wu, S. K., Zeng, K., Wilson, I. A., and Balch, W. E. (1996) *Trends. Biochem. Sci. 21*, 472−476.
30. Hansen, J. C., Lebowitz, J., and Demeler, B. (1994) *Biochemistry 33*, 13155−13163.
31. Seabra, M. C., Ho, Y. K., and Anant, J. S. (1995) *J. Biol. Chem. 270*, 24420−24427.
32. Schweins, T., and Wittinghofer, A. (1994) *Curr. Biol. 4*, 547−550.
33. Rost, B., and Sander, C. (1994) *Proteins 19*, 55−72.
34. Desnoyers, L., and Seabra, M. C. (1998) *Proc. Natl. Acad. Sci. U.S.A.* (in press).

BI980881A